HHS Public Access

Author manuscript

Biochim Biophys Acta Biomembr. Author manuscript; available in PMC 2024 August 01.

Published in final edited form as:

Biochim Biophys Acta Biomembr. 2023 August ; 1865(6): 184161. doi:10.1016/j.bbamem.2023.184161.

Impact of Ca^{2+} on Membrane Catalyzed IAPP Amyloid Formation and IAPP Induced Vesicle Leakage

Ming-Hao Li[1], **Xiaoxue Zhang**[2], **Erwin London**[1,2,3,*], **Daniel P. Raleigh**[1,2,4,*]

[1]Graduate Program in Biochemistry and Structural Biology, Stony Brook University, Stony Brook, New York 11794, United States

[2]Department of Chemistry, Stony Brook University, Stony Brook, New York 11794, United States

[3]Department of Biochemistry and Cell Biology, Stony Brook University, Stony Brook, New York 11794, United States

[4]Laufer Center for Physical and Quantitative Biology, Stony Brook University, Stony Brook, New York 11794, United States

Abstract

Human islet amyloid polypeptide (hIAPP, also known as amylin) is a 37 amino acid pancreatic polypeptide hormone that plays a role in regulating glucose levels, but forms pancreatic amyloid in type-2 diabetes. The process of amyloid formation by hIAPP contributes to β-cell death in the disease. Multiple mechanisms of hIAPP induced toxicity of β-cells have been proposed including disruption of cellular membranes. However, the nature of hIAPP membrane interactions and the effect of ions and other molecules on hIAPP membrane interactions are not fully understood. Many studies have used model membranes with a high content of anionic lipids, often POPS, however the concentration of anionic lipids in the β-cell plasma membrane is low. Here we study the concentration dependent effect of Ca^{2+} (0 to 50 mM) on hIAPP membrane interactions using large unilamellar vesicles (LUVs) with anionic lipid content ranging from 0 to 50 mole %. We find that Ca^{2+} does not effectively inhibit hIAPP amyloid formation and hIAPP induced membrane leakage from binary LUVs with a low percentage of POPS, but has a greater effect on LUVs with a high percentage of POPS. Mg^{2+} had very similar effects and the effects of Ca^{2+} and Mg^{2+} can be largely rationalized by the neutralization of POPS charge. The implications for hIAPP-membrane interactions are discussed.

[*]Authors to whom correspondence should be addressed: DPR daniel.raleigh@stonybrook.edu, phone: (631) 632-9547; EL erwin.london@stonybrook.edu, phone: (631) 632-8564.

Declaration of competing interest.

The authors declare that they have no known competing financial interests or personal relationships that could have appeared to influence the work reported in this paper.

CRediT authorship contribution statement

Ming-Hao Li: Conceptualization, Methodology, Formal Analysis, Visualization, Investigation, Writing - Original Draft **Xiaoxue Zhang:** Conceptualization, Investigation, Formal Analysis **Erwin London:** Conceptualization, Writing - Original Draft, Writing - Review & Editing, Supervision, Project administration, Funding Acquisition **Daniel Raleigh:** Conceptualization, Writing - Original Draft, Writing - Review & Editing, Supervision, Project administration, Funding Acquisition

Keywords

Amylin; Amyloid; Islet Amyloid Polypeptide; LUV; Peptide-Membrane Interactions

1. Introduction

Human islet amyloid polypeptide (hIAPP, also known as amylin) is a 37 amino acid pancreatic polypeptide hormone that is co-secreted with insulin from the pancreatic β-cell[1–6]. hIAPP plays a role in regulating glucose levels, but forms pancreatic amyloid in type-2 diabetes (T2D). The process of amyloid formation by hIAPP contributes to β-cell death in the pre-diabetic state and in T2D[1, 2, 7–11]. Multiple mechanisms of hIAPP induced toxicity of β-cells have been proposed including disruption of cellular membranes[9, 12–20]. However, the nature of hIAPP membrane interactions and the effect of ions and other molecules on hIAPP membrane interactions are not completely understood. Simple model systems have been widely used to study the interaction of hIAPP and membranes and have provided considerable insights. These investigations have shown that membrane composition impacts both hIAPP amyloid formation and the ability of hIAPP to induce membrane leakage[21–26]. Many experiments have used vesicles that contain high concentrations of anionic lipids, typically between 25 to 50 mole % anionic lipid or even higher. However, the concentration of anionic lipids in the β-cell plasma membrane is modest. The β-cell plasma membrane is asymmetric and is estimated to contain between 0.6 and 11 mole % of anionic lipid, mainly in the inner leaflet[22, 27]. This is an important consideration since hIAPP is a cationic polypeptide, and membranes with a higher percentage of anionic lipids are more effective at promoting hIAPP amyloid formation than those with a low percentage of anionic lipids. hIAPP is also more effective at inducing leakage of simple model membranes that contain a significant amount of anionic lipids. [13, 15–17, 21, 23, 28–31].

The primary sequence of hIAPP is displayed in Fig. 1[6, 32]. The peptide contains a disulfide bond between Cys-2 and Cys-7, has no acidic residues and the C-terminus is amidated. Depending on the exact pKa of the N-terminus and of the single His residue, the charge state of the peptide ranges from +2 to +4 at pH 7.4, and the peptide is positively charged at all physiologically relevant pH values.

Ca^{2+} flux is important for β-cell function[33–37] and Ca^{2+} has the potential to alter IAPP-membrane interactions at least *in vitro*[38–40]. This could be due to Ca^{2+} effects on the biophysical properties of membranes, particularly those with anionic lipids. Ca^{2+} is known to bind to the POPS headgroup and modulate the properties of POPS rich model membranes[41]. Important early work described the effects of 0 to 400 μM Ca^{2+} on IAPP interactions with model membranes that contain 30 mole % anionic lipids[38]. Ca^{2+} was observed to inhibit hIAPP membrane insertion and decreased hIAPP induced membrane leakage[38]. β-cell plasma membranes have anionic lipid content noticeably lower than 30 mole %[22], and physiological extracellular Ca^{2+} concentrations are in the low millimolar range while intracellular concentrations are in the 100 nanomolar range[33, 36, 42]. Therefore, studies of the effects of Ca^{2+} upon hIAPP membrane interactions under

a wide range of conditions, including those close to physiological, are of interest. Here we examine the effects of varying the Ca^{2+} concentration from 0 to 50 mM on the interactions of hIAPP with binary LUVs that contain varying concentration of POPS (0 to 50 mole %), and on LUVs that contain cholesterol.

Our experiments confirm that Ca^{2+} inhibits amyloid formation and IAPP induced membrane permeability of binary large unilamellar vesicles (LUVs) containing a high percentage of POPS for relatively high Ca^{2+} concentrations. Comparison to our previous studies suggests the effects of Ca^{2+} can be explained by the neutralization of PS charge[21]. Experiments using Mg^{2+} are consistent with this hypothesis. We find that physiological Ca^{2+} levels do not strongly inhibit hIAPP amyloid formation in the presence of binary LUVs containing POPC and a low percentage of POPS under the conditions of the assays. Permeability assays show that the effect of physiological Ca^{2+} levels on hIAPP induced membrane leakage from LUVs is reduced at lower percentages of POPS.

2. Methods and Materials

2.1. Materials:

1-palmitoyl-2-oleoyl-sn-glycero-3-phospho-L-serine (sodium salt) (POPS), 1-palmitoyl-2-oleoyl-glycero-3-phosphocholine (POPC), 1,2-dioleoyl-sn-glycero-3-phosphoethanolamine-N-(7-nitro-2-1,3-benzoxadiazol-4-yl) (NBD-POPE), 1,2-dioleoyl-sn-glycero-3-phosphoethanolamine-N-(lissamine rhodamine B sulfonyl) (Rh-DOPE) were purchased from Avanti Polar Lipids. Chelex-100, 5(6)-carboxyfluorescein, diphenylhexatriene (DPH), Triton X-100, dimethyl sulfoxide (DMSO), 1,1,1,3,3,3-hexafluoro-2-propanol (HFIP) and thioflavin-T were purchased from Sigma-Aldrich. The concentration of thioflavin-T was determined by absorbance at 412 nm, ε=36,000 $M^{-1}cm^{-1}$. Chloride salts of metal ions were used.

2.2. Preparation of large unilamellar vesicles (LUVs):

Lipids were initially dissolved in chloroform. The lipid mixture was dried by a stream of nitrogen and then under vacuum for one hour. Ca^{2+} was removed from DDI water using Chelex-100 (0.43g/liter) and decanting the water slowly from the resin before buffer preparation. Multilamellar vesicles were prepared by dissolving the dry lipid mixture in buffer (20 mM Tris, 100 mM NaCl, pH 7.4 with the desired Ca^{2+} concentration) and incubating in a 55°C water bath shaker for 30 minutes. LUVs were prepared by 7 freeze-thaw cycles and extrusion 11 times with a 100 nm pore polycarbonate membrane. To prepare LUVs for membrane permeability assays, the same method was used except the dry lipid film was dissolved in 80 mM carboxyfluorescein, 20 mM Tris, 100 mM NaCl, pH 7.4 buffer. Free carboxyfluorescein was removed using a PD-10 desalting column. The final lipid concentration was determined by the method of Stewart[43].

2.3. Peptide synthesis and purification:

hIAPP was synthesized using Fmoc chemistry with a CEM Liberty microwave peptide synthesizer at a 0.10 mmole scale. Fmoc-PAL-PEG-PS resin was used to provide C-terminal amidation. Fmoc-protected pseudoproline di-peptides were used at positions 9–10, 19–20,

and 27–28 to improve synthesis efficiency[44, 45]. All pseudoprolines, Arg, and β-branch amino acids were double coupled. His and Cys were coupled at a reduced temperature, 50°C, to reduce the level of racemization[45]. The peptide was cleaved from the resin using standard TFA methods. The crude peptide was dissolved in 20% acetic acid and lyophilized prior to purification. The disulfide bond was formed by dissolving the crude peptide in 100% DMSO and allowing it to sit at room temperature for three days. Formation of the disulfide bond was monitored by reverse phase analytical HPLC. The oxidized peptide was purified via reverse phase HPLC with a Proto 300 C18 preparative column and a two-buffer system. Buffer A contained 100% H_2O, and 0.045% of HCl. Buffer B contained 20% H_2O, 80% acetonitrile, and 0.045% of HCl. A Bruker AutoFlex II MALDI-TOF/TOF mass spectrometer was used to determine the molecular weight of the purified product: observed= 3903.3, expected =3902.7. Purified peptide was lyophilized and stored at −20 °C.

2.4. Membrane permeability assays:

LUVs loaded with 80 mM carboxyfluorescein were mixed with empty LUVs of the same composition so that 5% of the LUVs contained carboxyfluorescein. This was done to minimize changes in inner filter effects which can result from the release of the dye. LUV with a 400 μM total lipid concentration and 20 μM of hIAPP were loaded into a 96 well quartz plate. Fluorescence of carboxyfluorescein was measured using a DTX 880 plate reader at 25°C (excitation wavelength: 485 nm, and emission wavelength: 535 nm). The % fluorescence change was calculated as follows:

$$\text{fluorescence change}\,(\%) = (F(t)\text{-}Fmin)/(Fmax\text{-}Fmin) \times 100 \quad (1)$$

Where $F(t)$ is the fluorescence intensity of the carboxyfluorescein/hIAPP mixture at a given time t, $Fmin$ is the fluorescence intensity of the LUV without hIAPP added, and $Fmax$ is the fluorescence intensity of fully disrupted LUV, achieved by the addition of 2 mole % of triton x-100. The % fluorescence is directly related to the % of carboxyfluorescein leakage provided there are no significant inner filter effects[21, 28].

2.5. Amyloid formation assays:

Thioflavin-T measurements were made in 20 mM Tris, 100 mM NaCl buffer at pH 7.4. Thioflavin-T was mixed with hIAPP in buffer immediately before the experiment and the samples were then loaded into a 96 well quartz plate. The final concentration of thioflavin-T and hIAPP were 40 μM and 20 μM, respectively. Fluorescence of thioflavin-T was monitored using a DTX 880 plate reader (excitation wavelength: 430 nm, and emission wavelength: 485 nm). Readings were made every 10 minutes with no additional shaking. T_{50} is the time to reach half-maximum fluorescence intensity.

2.6. Fluorescence anisotropy measurements:

0.1 μM of DPH and LUVs with 100 μM total lipid were used for the fluorescence anisotropy experiments. DPH was dissolved in ethanol, added to LUV solution, and incubated at room temperature for 5 minutes before anisotropy experiments. The vertical and horizontal

fluorescence intensity of DPH was measured using a SPEX automated Glan-Thompson polarizer accessory. Anisotropy was calculated using the equation:

$$R = (I_{VV} - G*I_{VH})/(I_{VV} + 2G*I_{VH}) \quad (2)$$

where I_{VV} and I_{VH} are the parallel and perpendicular polarized fluorescence intensity with vertically polarized fluorescence excitation, and G is the correction factor = I_{HV}/I_{HH}.

2.7. FRET-based quenching assays of vesicle fusion:

Vesicles with a FRET donor lipid, 0.5 mole % nitrobenzoxadiazole-DOPE (NBD-DOPE), and a FRET acceptor lipid, 1 mole % rhodamine-DOPE (Rh-DOPE) lipids were used. The fluorescence-labeled LUV and unlabeled LUV were mixed in a 1:9 ratio and loaded into a 96-well quartz plate. Fluorescence was excited at 463 nm and recorded at 536 nm using a Molecular Devices Gemini EM plate reader. The calcium stock solution was 5 M $CaCl_2$. Samples without calcium were loaded into the plate and then calcium was added (calcium injection). Fluorescence measured in buffer without LUVs was monitored to give the minimum fluorescence intensity, and LUVs mixed with 2 mole % of triton x-100 were used to give the maximum fluorescence intensity.

2.8. Transmission electron microscopy (TEM):

Samples were prepared by blotting 15 uL of material collected at the end of the thioflavin-T kinetic assays onto Carbon-coated Formvar 300 mesh copper grids. The same volume of 1% depleted uranyl acetate was used to negatively stain each sample. Images were taken at the Central Microscopy Imaging Center at Stony Brook University.

2.9. Circular Dichroism (CD):

CD spectra were recorded at 25 °C using a Jasco J-715 CD spectrometer and 0.1 cm cells. Spectra were recorded over the wavelength range of 260 to 195 nm in 1 nm steps.

3. Results and discussion

3.1. The rate of hIAPP amyloid formation in the presence of LUVs decreases with increasing Ca^{2+} ion concentration, but the effect is not significant for vesicles containing low mole % POPS

We began with studies of binary LUVs containing POPS and POPC, chosen in part because prior work has used binary systems that contain an anionic and a zwitterionic phospholipid. We first tested the effect of adding $CaCl_2$ on the kinetics of hIAPP amyloid formation in the absence of vesicles. Amyloid formation was monitored using fluorescence-based thioflavin-T assays. These have been widely applied to studies of hIAPP amyloid formation in homogeneous solution and in the presence of LUVs and other model membranes. There was no detectable change in the time course of thioflavin-T time fluorescence increase with the addition of 1 mM $CaCl_2$ and, at most, only a very modest effect with 10 mM $CaCl_2$ (Fig. S1). However, addition of 50 mM $CaCl_2$ reduced the T_{50} by 60%. The effect is likely due to the change in ionic strength. Addition of 50 mM $CaCl_2$ increases the ionic strength by

150 mM and hIAPP amyloid formation is known to be accelerated by an increase in ionic strength in this range [46].

The effect of Ca^{2+} on LUV catalyzed hIAPP amyloid formation was examined for binary LUVs with various amounts of POPS (anionic lipid) and POPC (zwitterionic lipid), ranging from 0 mole % POPS to 50 mole % POPS (Fig. 2A, Table S1, and Fig. S2). This spans the range from physiologically relevant POPS levels to the much higher values commonly employed in biophysical studies. Amyloid formation was monitored by thioflavin-T assays. Prior studies have shown that thioflavin-T assays accurately report on the kinetics of hIAPP under a wide range of conditions. However, thioflavin-T is an extrinsic probe and it is important to verify the results with other methods. We used transmission electron microscopy (TEM) to confirm the presence of amyloid fibrils. (Fig. S3, and Fig. S10). We also used CD spectroscopy to confirm the transition to β-sheet structure (Fig. S4).

Fig. 2A compares the value of T_{50} with and without 1 mM Ca^{2+} as a function of the mole % POPS. Fig. 2B displays a plot of the ratio of T_{50} in the presence and in the absence of Ca^{2+}. Increasing POPS accelerates amyloid formation, as expected from prior studies. This was true both with and without Ca^{2+}. In contrast to the effect of Ca^{2+} in the absence of LUVs, Ca^{2+} partially inhibits amyloid formation in the presence of binary LUVs containing POPS, as in previous studies[21, 38]. The magnitude of the effect depends on the amount of POPS in the LUV. At low POPS concentrations, (< 5 mole %), 1 mM Ca^{2+} had a noticeably smaller effect on the rate of hIAPP amyloid formation than at higher POPS concentrations. For example, addition of 1 mM Ca^{2+} leads to a 2.8-fold increase in T_{50} in the presence of LUVs containing 25 or 50 mole % POPS, but only a 1.6-fold increase for samples that contain LUVs with 5 mole % POPS. An even smaller increase in T_{50}, just 40%, was detected for the LUVs containing 2 mole % POPS (Fig. 2, Table S1). The difference in the direction of the effect of Ca^{2+} upon amyloid formation in the presence and absence of LUV shows that the effect of Ca^{2+} in the presence of vesicles is not due to Ca^{2+} effects upon ionic strength since increases in ionic strength accelerate hIAPP amyloid formation in aqueous solution in the absence of vesicles.

The above experiments were conducted using a lipid to peptide ratio of 20:1 (400 μM lipid and 20 μM peptide). We repeated the kinetics assays using a higher (100:1) lipid to peptide ratio for LUVs comprised of 100% POPC and for LUVs made up of 75 mole % POPC, 25 mole % POPS (Fig. S5, Table S2). Similar Ca^{2+} dependent effects were observed. For the pure POPC LUVs (no POPS), no change in T_{50} was detected when 1 mM Ca^{2+} was added. For the 25 mole % POPS, 75 mole % POPC LUVs, T_{50} was increased 2-fold upon addition of 1 mM Ca^{2+}.

3.2. Calcium inhibition of LUV mediated amyloid formation saturates at ~10 mM Ca^{2+} for binary LUVs containing 10 mole % POPS, 400 μM lipid, and 20 μM hIAPP

We next studied the effect of varying the Ca^{2+} concentration on hIAPP membrane-mediated amyloid formation. Ca^{2+} is known to induce membrane fusion and it is important to control for these effects[47–52]. We wished to avoid vesicle fusion which increases vesicle size and might affect interactions with hIAPP. Thus, we first conducted control experiments to test what range of Ca^{2+} ion concentrations and POPS content lead to vesicle-fusion. A

FRET-based assay with NBD-DOPE (donor) and Rh-DOPE (acceptor) labeled fluorescence lipids was used. Binary LUVs with 10 mole % POPS and 50 mole % POPS were tested (Fig. S6). In the absence of fusion, the fluorescence of NBD-DOPE is low because it is quenched by the Rh-DOPE. If fusion occurs between labeled vesicles and vesicles without FRET donor and acceptor, the concentration of Rh-DOPE in the vesicle decreases and consequently the NBD-DOPE fluorescence increases. Ca^{2+} was injected into solutions of mixed 1:9 fluorescence labeled and unlabeled LUV at time 0 (Fig. S6). The data shows that for the binary LUVs with high POPS content (50 mole % POPS), Ca^{2+} induces vesicle fusion even for relatively low Ca^{2+} ion concentrations (5 mM $CaCl_2$) (Fig. S6A). However, no fusion was observed for LUVs containing 10 mole % or lower POPS even at the highest injected Ca^{2+} ion concentration (50 mM $CaCl_2$) (Fig. S6B).

Based on the control experiments, we used binary LUVs made up of 10 mole % POPS, 90 mole % POPC to study the effect of higher Ca^{2+} concentrations on hIAPP amyloid formation (Fig. 3 and Fig. S7). Data normalized on the Y-axis are displayed in figure 3 and the unnormalized data in supporting Fig. S7. Fiber formation was confirmed using TEM (Fig. S3). The T_{50} for amyloid formation increased as Ca^{2+} concentration increased, and the effect saturated between 10 mM and 50 mM of Ca^{2+}. At 10 mM Ca^{2+}, the T_{50} was 2.7-fold larger than in the absence of Ca^{2+}.

Examination of the unnormalized data (Fig S7) reveals that the final thioflavin-T intensities are similar except for the experiment conducted with 50 mM $CaCl_2$. In that case the final intensity is reduced. It is difficult to correlate the final intensity in thioflavin-T assays conducted under different conditions with the amount of amyloid formed. Fibrils formed under different conditions can adopt different structures and their lateral association might be altered. This can affect the affinity of the thioflavin-T for the fibrils, the number of binding sites, or the structure of the bound thioflavin-T. The latter is important because the quantum yield of thioflavin-T is sensitive to the details of its bound structure.

3.3. Calcium inhibits hIAPP induced membrane leakage, but the effects depend on the POPS content

We next examined the effects of added Ca^{2+} on hIAPP induced membrane leakage. Membrane permeability was studied using a dye-based leakage assay. High concentrations (80 mM) of carboxyfluorescein were encapsulated in the binary LUVs. The high concentration leads to self-quenching of carboxyfluorescein fluorescence, while hIAPP induced leakage of carboxyfluorescein from the LUVs reduces the self-quenching and leads to an increase in fluorescence[21]. The measurements were conducted using samples in which 5% of the LUVs contained dye and the reminder did not in order to reduce any changes in fluorescence due to changes in inner filter effects caused by dye release. Binding of Ca^{2+} to the LUVs inhibited, but did not eliminate hIAPP induced membrane leakage and the effect was more pronounced at high POPS mole %. Differences were observed at both early (10 minutes) and late times (20 hours) (Fig. 4, and Fig. S8). For example, at 50 mole % POPS, the addition of 1 mM Ca^{2+} reduced hIAPP induced leakage from 77 ± 3.8 to 51 ± 2.4 % at 10 minutes and from 97 ± 4.3 to 77 ± 2.9 % at 20 hours. For 2 mole % POPS, the addition of the same Ca^{2+} concentration modestly reduced hIAPP induced leakage from 30

± 0.6 to 26.0 ± 0.4 % at 10 minutes and from 50 ± 2.8 to 47 ± 1.2 at 20 hours (Table S3). Notice that significant leakage is still observed in the presence of Ca^{2+}.

3.4. Calcium inhibits hIAPP induced membrane leakage in a concentration dependent manner

We next examined the hIAPP induced leakage of LUVs containing 10 mole % POPS, 90 mole % POPC as a function of Ca^{2+} (Fig. 5). hIAPP induced leakage was reduced as the Ca^{2+} concentration increased, and the effect saturated between 10 mM and 50 mM Ca^{2+}, a similar result to what we observed for the inhibition of amyloid formation. The amount of leakage observed at 10 minutes was reduced from 66 % in the absence of Ca^{2+} to 25% in the presence of 10 mM Ca^{2+} (Fig. 5) A significant reduction was also observed at late times (20 hours): from 77% without Ca^{2+} to 34% with 10 mM Ca^{2+}.

3.5. Mg^{2+} impacts hIAPP amyloid formation and hIAPP induced LUV leakage in a similar fashion to Ca^{2+}

Ca^{2+} is known to interact with POPS headgroups via electrostatic interactions. If electrostatic interactions play a significant role in the effects observed here, then Mg^{2+} should influence leakage and amyloid formation in a similar fashion. Consequently, we repeated the experiments for the 10 mole % POPS, 90 mole % POPC LUVs using Mg^{2+} instead of Ca^{2+}. Mg^{2+} led to slower amyloid formation and less leakage, and the effects were virtually identical to those observed with Ca^{2+} (Fig. 6). We also examined the effects of added Zn^{2+}. The limited solubility of $ZnCl_2$. precluded an in-depth concentration dependent study. Addition of 1 mM $ZnCl_2$ has similar effect as the addition of 1 mM $MgCl_2$ (Fig. S9). Zn^{2+} is known to have complicated pH and concentration dependent effects on amyloid formation by hIAPP[53–57]. We did not conduct a detailed concentration dependent study because of these considerations, and because of the limited solubility of $ZnCl_2$, and because the focus here is on Ca^{2+} dependent interactions.

3.6. Ca^{2+} also slows amyloid formation for LUVs which contain cholesterol

Cell membranes contain cholesterol and the presence of cholesterol in LUVs is known to impact LUV mediated hIAPP amyloid[21, 28]. We tested if Ca^{2+} impacts membrane mediated amyloid formation for LUVs composed of 10 mole % POPS, 50 mole % POPC, and 40 mole % cholesterol (Fig. 7, Fig. S10). As expected, hIAPP amyloid formation was slower in the presence of LUVs containing cholesterol than in the presence of LUVs without cholesterol in the absence of Ca^{2+}. Addition of Ca^{2+} led to larger T_{50} values for the cholesterol-containing LUV indicating the Ca^{2+} also slowed amyloid formation for this system. Addition of 10 mM led to a 3-fold increase in T_{50}. At the highest Ca^{2+} tested, 50mM, the T_{50} was larger than the value observed in the absence of Ca^{2+}, but is less than the value observed for 10 mM Ca^{2+}. This is different than the results observed for the LUVs which lacked cholesterol. In that case, addition of Ca^{2+} lead to a monotonic increase in T_{50}. This may reflect competing effects in solution and on the vesicles' surface. In solution, 50 mM $CaCl_2$ led to a reduction in T_{50} (faster amyloid formation). Cholesterol weakens hIAPP membrane interactions and it may be that cholesterol and high Ca^{2+} together led to even weaker interaction. In this scenario, a larger fraction of the peptide could form amyloid in solution under these conditions. Irrespective of the details, the critical observation is that

Ca^{2+} above 1 mM slowed amyloid formation for cholesterol containing LUVs with 10% POPS (Fig. 7, Fig. S10).

3.7. The effect of calcium on membrane fluidity as judged by diphenylhexatriene (DPH) anisotropy

Prior work has shown that the fluidity of model membranes affects the rate of LUV catalyzed hIAPP amyloid formation[28]. We tested if the effects of Ca^{2+} on amyloid formation and membrane permeability observed here correlate with changes in membrane fluidity/order, using fluorescence anisotropy measurements of DPH containing LUVs. DPH fluorescence anisotropy of DPH in membranes reports on the extent of rotation, a parameter limited by membrane order[58–63]. We titrated Ca^{2+} from 0 to 50 mM for LUVs containing 10, 25, and 50 mole % POPS (Table S4). We observed no significant change in DPH fluorescence anisotropy (which can be as high as 0.30 when a membrane is in an ordered state[64]). For example, with 10 mole % POPS, the DPH anisotropy was 0.10 ± 0.01 at 0 mM Ca^{2+}, 0.11 ± 0.01 at 10 mM Ca^{2+}, and 0.11 ± 0.01 at 50 mM Ca^{2+}. For 50 mole % POPS, the DPH anisotropy was 0.11 ± 0.01 at 0 mM Ca^{2+}, 0.12 ± 0.01 at 10 mM Ca^{2+}, and 0.12 ± 0.01 at 50 mM Ca^{2+} (Table S4). Prior work has shown that Ca^{2+} does not induce phase separation with formation of ordered domains for 10 mole % POPS[65]. That observation, together with the current result indicates no significant increase in rigidification/order occurs upon addition of Ca^{2+} to the LUVs containing 0 and 10 mole % POPS under the conditions of our experiments as monitored by DPH anisotropy. The data for higher mole % POPS is harder to interpret. There are two possibilities: If phase separation does not occur, the anisotropy measurement indicated no detectable rigidification. However, if phase separation is induced, it is possible the DPH probe is excluded from the more rigid POPS: Ca^{2+} domains, so that there could be an increase in membrane order that DPH is unable to detect. The work reported by Silvius[65] has shown that phase separation is induced by Ca^{2+} in multilamellar systems for POPS concentration of 25 mole % and above. While different from the systems used here, this early work suggests that phase separation is likely and, if so, our data suggests that the DPH phase is excluded from the POPS: Ca^{2+} phase.

4. Conclusions

The presence of POPS in model membranes accelerates amyloid formation and increases hIAPP induced membrane leakage. This appears to be related to the negative charge on the POPS molecules[21]. Thus, the reduction of amyloid formation and leakiness by Ca^{2+} for the model membranes used here is consistent with charge neutralization of the POPS headgroup. The Mg^{2+} studies support this hypothesis.

The data reported here shows that the effects of Ca^{2+} on the rate of amyloid formation and on the ability of hIAPP to induce leakage depends on the amount of POPS contained within the model membrane. The observed effects saturate somewhere between 10 and 50 mM Ca^{2+} which is broadly consistent with early studies of Ca^{2+} binding to POPS containing membranes[41]. Modest effects are observed at the lower POPS values that fall in the physiological range compared to the higher POPS concentrations. The results show that

Ca^{2+} effects on hIAPP model membrane interactions are a strong function of the amount of POPS in the model membrane, and highlights the important role of POPS in Ca^{2+} dependent effects in such systems. The data shows that Ca^{2+} also has effects on cholesterol containing LUVs which contain POPS. The time to form amyloid is longer for LUVs that contain cholesterol. These observations are in good agreement with prior results[21, 28]. The addition of Ca^{2+} further lengthens the time to form amyloid for the cholesterol containing LUVs.

It is difficult to extrapolate from the experimental data reported here even at low POPS mole % to the relevant biological membrane since those contain a complicated mixture of lipids and are asymmetric. However, consideration of plasma membrane composition and the extra and intercellular Ca^{2+} levels together with the data presented here argues that Ca^{2+} induced modulation of the physical properties of the plasma membrane is unlikely to affect hIAPP plasma membrane interactions significantly *in vivo*. If hIAPP amyloid formation begins extracellularly, as has been proposed by some workers[3, 12, 66], the polypeptide will interact with the outer leaflet of the β-cell plasma membrane which has a very low mole % of anionic lipids. The data presented here shows that added Ca^{2+} has very modest effects for the model membranes which contain a low mole % of anionic lipids. Some workers have proposed that hIAPP fibrils may have an intracellular origin, but even the inner leaflet of the β-cell plasma membrane is estimated to contain a % of POPS that is lower than used in most biophysical studies[22]. In addition, intracellular Ca^{2+} concentrations are much lower than extracellular concentrations and are in 100s of nanomolar range.[33, 37, 42]. This suggests that Ca^{2+} modulation of the physical properties of the inner leaflet is also unlikely to play a significant role in modulating hIAPP interactions with the inner leaflet *in vivo*.

Supplementary Material

Refer to Web version on PubMed Central for supplementary material.

Acknowledgements

This work was supported by the National Institutes of Health (grant number GM078114, GM122493); National Science Foundation (grant MCB1715525); and a Seed Grant from the Stony Brook University Office of the Vice President for research.

Abbreviations

DMSO	dimethyl sulfoxide
DPH	diphenylhexatriene
HFIP	1,1,1,3,3,3-hexafluoro-2-propanol
hIAPP	human islet amyloid polypeptide
LUV	large unilamellar vesicle
MLV	multilamellar vesicles

NBD-POPE	1,2-dioleoyl-sn-glycero-3-phosphoethanolamine-N-(7-nitro-2-1,3-benzoxadiazol-4-yl)
POPC	1-palmitoyl-2-oleoyl-glycero-3-phosphocholine
POPS	1-palmitoyl-2-oleoyl-sn-glycero-3-phospho-L-serine (sodium salt)
Rh-DOPE	1,2-dioleoyl-sn-glycero-3-phosphoethanolamine-N-(lissamine rhodamine B sulfonyl)
T2D	type-2 diabetes

References:

[1]. Hay DL, Chen S, Lutz TA, Parkes DG, Roth JD, Amylin: pharmacology, physiology, and clinical potential, Pharmacol Rev, 67 (2015) 564–600. [PubMed: 26071095]

[2]. Westermark P, Wernstedt C, Wilander E, Hayden DW, O'Brien TD, Johnson KH, Amyloid fibrils in human insulinoma and islets of Langerhans of the diabetic cat are derived from a neuropeptide-like protein also present in normal islet cells, Proc Natl Acad Sci U S A, 84 (1987) 3881–3885. [PubMed: 3035556]

[3]. Akter R, Cao P, Noor H, Ridgway Z, Tu LH, Wang H, Wong AG, Zhang X, Abedini A, Schmidt AM, Raleigh DP, Islet amyloid polypeptide: structure, function, and pathophysiology, J Diabetes Res, 2016 (2016) 2798269. [PubMed: 26649319]

[4]. Westermark P, Andersson A, Westermark GT, Islet amyloid polypeptide, islet amyloid, and diabetes mellitus, Physiol Rev, 91 (2011) 795–826. [PubMed: 21742788]

[5]. Lutz TA, The role of amylin in the control of energy homeostasis, Am J Physiol Regul Integr Comp Physiol, 298 (2010) R1475–R1484. [PubMed: 20357016]

[6]. Cooper GJ, Willis AC, Clark A, Turner RC, Sim RB, Reid KB, Purification and characterization of a peptide from amyloid-rich pancreases of type 2 diabetic patients, Proc Natl Acad Sci U S A, 84 (1987) 8628–8632. [PubMed: 3317417]

[7]. Abedini A, Plesner A, Cao P, Ridgway Z, Zhang J, Tu LH, Middleton CT, Chao B, Sartori DJ, Meng F, Wang H, Wong AG, Zanni MT, Verchere CB, Raleigh DP, Schmidt AM, Time-resolved studies define the nature of toxic IAPP intermediates, providing insight for anti-amyloidosis therapeutics, Elife, 5 (2016) 12977.

[8]. Raleigh D, Zhang X, Hastoy B, Clark A, The beta-cell assassin: IAPP cytotoxicity, J Mol Endocrinol, 59 (2017) R121–R140. [PubMed: 28811318]

[9]. Abedini A, Schmidt AM, Mechanisms of islet amyloidosis toxicity in type 2 diabetes, FEBS Lett, 587 (2013) 1119–1127. [PubMed: 23337872]

[10]. Hull RL, Westermark GT, Westermark P, Kahn SE, Islet amyloid: A critical entity in the pathogenesis of type 2 diabetes, J Clin Endocrinol Metab, 89 (2004) 3629–3643. [PubMed: 15292279]

[11]. Blencowe M, Furterer A, Wang Q, Gao F, Rosenberger M, Pei L, Nomoto H, Mawla AM, Huising MO, Coppola G, Yang X, Butler PC, Gurlo T, IAPP-induced beta cell stress recapitulates the islet transcriptome in type 2 diabetes, Diabetologia, 65 (2022) 173–187. [PubMed: 34554282]

[12]. Janson J, Ashley RH, Harrison D, McIntyre S, Butler PC, The mechanism of islet amyloid polypeptide toxicity is membrane disruption by intermediate-sized toxic amyloid particles, Diabetes, 48 (1999) 491–498. [PubMed: 10078548]

[13]. Anguiano M, Nowak RJ, Lansbury PT Jr., Protofibrillar islet amyloid polypeptide permeabilizes synthetic vesicles by a pore-like mechanism that may be relevant to type II diabetes, Biochemistry, 41 (2002) 11338–11343. [PubMed: 12234175]

[14]. Weise K, Radovan D, Gohlke A, Opitz N, Winter R, Interaction of hIAPP with model raft membranes and pancreatic beta-cells: cytotoxicity of hIAPP oligomers, Chembiochem, 11 (2010) 1280–1290. [PubMed: 20440729]

[15]. Cao P, Abedini A, Wang H, Tu LH, Zhang X, Schmidt AM, Raleigh DP, Islet amyloid polypeptide toxicity and membrane interactions, Proc Natl Acad Sci U S A, 110 (2013) 19279–19284. [PubMed: 24218607]

[16]. Engel MF, Membrane permeabilization by islet amyloid polypeptide, Chem Phys Lipids, 160 (2009) 1–10. [PubMed: 19501206]

[17]. Brender JR, Salamekh S, Ramamoorthy A, Membrane disruption and early events in the aggregation of the diabetes related peptide IAPP from a molecular perspective, Acc Chem Res, 45 (2012) 454–462. [PubMed: 21942864]

[18]. Sciacca MF, Lolicato F, Tempra C, Scollo F, Sahoo BR, Watson MD, Garcia-Vinuales S, Milardi D, Raudino A, Lee JC, Ramamoorthy A, La Rosa C, Lipid-chaperone hypothesis: a common molecular mechanism of membrane disruption by intrinsically disordered proteins, ACS Chem Neurosci, 11 (2020) 4336–4350. [PubMed: 33269918]

[19]. Milardi D, Gazit E, Radford SE, Xu Y, Gallardo RU, Caflisch A, Westermark GT, Westermark P, Rosa C, Ramamoorthy A, Proteostasis of islet amyloid polypeptide: a molecular perspective of risk factors and protective strategies for type II diabetes, Chem Rev, 121 (2021) 1845–1893. [PubMed: 33427465]

[20]. Pathak BK, Dey S, Mozumder S, Sengupta J, The role of membranes in function and dysfunction of intrinsically disordered amyloidogenic proteins, Adv Protein Chem Struct Biol, 128 (2022) 397–434. [PubMed: 35034725]

[21]. Zhang X, St Clair JR, London E, Raleigh DP, Islet amyloid polypeptide membrane interactions: effects of membrane composition, Biochemistry, 56 (2017) 376–390. [PubMed: 28054763]

[22]. Seeliger J, Weise K, Opitz N, Winter R, The effect of abeta on IAPP aggregation in the presence of an isolated beta-cell membrane, J Mol Biol, 421 (2012) 348–363. [PubMed: 22321797]

[23]. Knight JD, Miranker AD, Phospholipid catalysis of diabetic amyloid assembly, J Mol Biol, 341 (2004) 1175–1187. [PubMed: 15321714]

[24]. Dignon GL, Zerze GH, Mittal J, Interplay between membrane composition and structural stability of membrane-bound hIAPP, J Phys Chem B, 121 (2017) 8661–8668. [PubMed: 28829144]

[25]. Saghir AE, Farrugia G, Vassallo N, The human islet amyloid polypeptide in protein misfolding disorders: Mechanisms of aggregation and interaction with biomembranes, Chem Phys Lipids, 234 (2021) 105010. [PubMed: 33227292]

[26]. Caillon L, Lequin O, Khemtemourian L, Evaluation of membrane models and their composition for islet amyloid polypeptide-membrane aggregation, Biochim Biophys Acta, 1828 (2013) 2091–2098. [PubMed: 23707907]

[27]. Turk J, Wolf BA, Lefkowith JB, Stump WT, McDaniel ML, Glucose-induced phospholipid hydrolysis in isolated pancreatic islets: quantitative effects on the phospholipid content of arachidonate and other fatty acids, Biochim Biophys Acta, 879 (1986) 399–409. [PubMed: 3535899]

[28]. Zhang X, London E, Raleigh DP, Sterol structure strongly modulates membrane-islet amyloid polypeptide interactions, Biochemistry, 57 (2018) 1868–1879. [PubMed: 29373018]

[29]. Jayasinghe SA, Langen R, Lipid membranes modulate the structure of islet amyloid polypeptide, Biochemistry, 44 (2005) 12113–12119. [PubMed: 16142909]

[30]. Khemtemourian L, Fatafta H, Davion B, Lecomte S, Castano S, Strodel B, Structural dissection of the first events following membrane binding of the islet amyloid polypeptide, Front Mol Biosci, 9 (2022) 849979. [PubMed: 35372496]

[31]. Gao M, Winter R, The effects of lipid membranes, crowding and osmolytes on the aggregation, and fibrillation propensity of human IAPP, J Diabetes Res, 2015 (2015) 849017. [PubMed: 26582333]

[32]. Westermark P, Wernstedt C, O'Brien TD, Hayden DW, Johnson KH, Islet amyloid in type 2 human diabetes mellitus and adult diabetic cats contains a novel putative polypeptide hormone, Am J Pathol, 127 (1987) 414–417. [PubMed: 3296768]

[33]. Bagur R, Hajnoczky G, Intracellular Ca(2+) sensing: Its role in calcium homeostasis and signaling, Mol Cell, 66 (2017) 780–788. [PubMed: 28622523]

[34]. Bronner F, Extracellular and intracellular regulation of calcium homeostasis, ScientificWorldJournal, 1 (2001) 919–925. [PubMed: 12805727]

[35]. Cascella R, Cecchi C, Calcium dyshomeostasis in Alzheimer's disease pathogenesis, Int J Mol Sci, 22 (2021) 4914. [PubMed: 34066371]

[36]. Weiser A, Feige JN, De Marchi U, Mitochondrial calcium signaling in pancreatic beta-Cell, Int J Mol Sci, 22 (2021) 2515. [PubMed: 33802289]

[37]. Zhang IX, Raghavan M, Satin LS, The endoplasmic reticulum and calcium homeostasis in pancreatic beta cells, Endocrinology, 161 (2020) bqz028. [PubMed: 31796960]

[38]. Sciacca MF, Milardi D, Messina GM, Marletta G, Brender JR, Ramamoorthy A, La Rosa C, Cations as switches of amyloid-mediated membrane disruption mechanisms: calcium and IAPP, Biophys J, 104 (2013) 173–184. [PubMed: 23332070]

[39]. Milardi D, Sciacca MF, Randazzo L, Raudino A, La Rosa C, The role of calcium, lipid membranes and islet amyloid polypeptide in the onset of type 2 diabetes: innocent bystanders or partners in a crime?, Front Endocrinol (Lausanne), 5 (2014) 216. [PubMed: 25566188]

[40]. Sciacca MFM, Tempra C, Scollo F, Milardi D, La Rosa C, Amyloid growth and membrane damage: Current themes and emerging perspectives from theory and experiments on Abeta and hIAPP, Biochim Biophys Acta Biomembr, 1860 (2018) 1625–1638. [PubMed: 29501606]

[41]. Duzgunes N, Nir S, Wilschut J, Bentz J, Newton C, Portis A, Papahadjopoulos D, Calcium- and magnesium-induced fusion of mixed phosphatidylserine/phosphatidylcholine vesicles: effect of ion binding, J Membr Biol, 59 (1981) 115. [PubMed: 7241577]

[42]. Bergsten P, Glucose-induced pulsatile insulin release from single islets at stable and oscillatory cytoplasmic Ca2+, Am J Physiol, 274 (1998) E796–800. [PubMed: 9612236]

[43]. Stewart JC, Colorimetric determination of phospholipids with ammonium ferrothiocyanate, Anal Biochem, 104 (1980) 10–14. [PubMed: 6892980]

[44]. Abedini A, Raleigh DP, Incorporation of pseudoproline derivatives allows the facile synthesis of human IAPP, a highly amyloidogenic and aggregation-prone polypeptide, Org Lett, 7 (2005) 693–696. [PubMed: 15704927]

[45]. Marek P, Woys AM, Sutton K, Zanni MT, Raleigh DP, Efficient microwave-assisted synthesis of human islet amyloid polypeptide designed to facilitate the specific incorporation of labeled amino acids, Org Lett, 12 (2010) 4848–4851. [PubMed: 20931985]

[46]. Marek PJ, Patsalo V, Green DF, Raleigh DP, Ionic strength effects on amyloid formation by amylin are a complicated interplay among Debye screening, ion selectivity, and Hofmeister effects, Biochemistry, 51 (2012) 8478–8490. [PubMed: 23016872]

[47]. Papahadjopoulos D, Nir S, Duzgunes N, Molecular mechanisms of calcium-induced membrane fusion, J Bioenerg Biomembr, 22 (1990) 157–179. [PubMed: 2139437]

[48]. Yaradanakul A, Wang TM, Lariccia V, Lin MJ, Shen C, Liu X, Hilgemann DW, Massive Ca-induced membrane fusion and phospholipid changes triggered by reverse Na/Ca exchange in BHK fibroblasts, J Gen Physiol, 132 (2008) 29–50. [PubMed: 18562498]

[49]. Allolio C, Harries D, Calcium Ions Promote Membrane Fusion by Forming Negative-Curvature Inducing Clusters on Specific Anionic Lipids, ACS Nano, 15 (2021) 12880–12887. [PubMed: 34338519]

[50]. Papahadjopoulos D, Vail WJ, Pangborn WA, Poste G, Studies on membrane fusion. II. Induction of fusion in pure phospholipid membranes by calcium ions and other divalent metals, Biochim Biophys Acta, 448 (1976) 265–283. [PubMed: 822885]

[51]. Churchward MA, Rogasevskaia T, Brandman DM, Khosravani H, Nava P, Atkinson JK, Coorssen JR, Specific lipids supply critical negative spontaneous curvature--an essential component of native Ca2+-triggered membrane fusion, Biophys J, 94 (2008) 3976–3986. [PubMed: 18227127]

[52]. Kachar B, Fuller N, Rand RP, Morphological responses to calcium-induced interaction of phosphatidylserine-containing vesicles, Biophys J, 50 (1986) 779–788. [PubMed: 3790685]

[53]. Brender JR, Hartman K, Nanga RP, Popovych N, de R la Salud Bea, S. Vivekanandan, E.N. Marsh, A. Ramamoorthy, Role of zinc in human islet amyloid polypeptide aggregation, J Am Chem Soc, 132 (2010) 8973–8983. [PubMed: 20536124]

[54]. Brender JR, Krishnamoorthy J, Messina GM, Deb A, Vivekanandan S, La Rosa C, Penner-Hahn JE, Ramamoorthy A, Zinc stabilization of prefibrillar oligomers of human islet amyloid polypeptide, Chem Commun (Camb), 49 (2013) 3339–3341. [PubMed: 23505632]

[55]. Salamekh S, Brender JR, Hyung SJ, Nanga RP, Vivekanandan S, Ruotolo BT, Ramamoorthy A, A two-site mechanism for the inhibition of IAPP amyloidogenesis by zinc, J Mol Biol, 410 (2011) 294–306. [PubMed: 21616080]

[56]. Khemtemourian L, Antoniciello F, Sahoo BR, Decossas M, Lecomte S, Ramamoorthy A, Investigation of the effects of two major secretory granules components, insulin and zinc, on human-IAPP amyloid aggregation and membrane damage, Chem Phys Lipids, 237 (2021) 105083. [PubMed: 33887213]

[57]. Lee YH, Lin Y, Cox SJ, Kinoshita M, Sahoo BR, Ivanova M, Ramamoorthy A, Zinc boosts EGCG's hIAPP amyloid Inhibition both in solution and membrane, Biochim Biophys Acta Proteins Proteom, 1867 (2019) 529–536. [PubMed: 30468883]

[58]. Dale RE, Chen LA, Brand L, Rotational relaxation of the "microviscosity" probe diphenylhexatriene in paraffin oil and egg lecithin vesicles, J Biol Chem, 252 (1977) 7500–7510. [PubMed: 914824]

[59]. Lentz BR, Membrane "fluidity" as detected by diphenylhexatriene probes, Chemistry and Physics of Lipids, 50 (1989) 171–190.

[60]. Kaiser RD, London E, Location of diphenylhexatriene (DPH) and its derivatives within membranes: comparison of different fluorescence quenching analyses of membrane depth, Biochemistry, 38 (1999) 2610.

[61]. Lentz BR, Use of fluorescent probes to monitor molecular order and motions within liposome bilayers, Chem Phys Lipids, 64 (1993) 99–116. [PubMed: 8242843]

[62]. London E, Feligenson GW, A convenient and sensitive fluorescence assay for phospholipid vesicles using diphenylhexatriene, Anal Biochem, 88 (1978) 203–211. [PubMed: 696996]

[63]. Chattopadhyay A, London E, Fluorimetric determination of critical micelle concentration avoiding interference from detergent charge, Anal Biochem, 139 (1984) 408–412. [PubMed: 6476378]

[64]. Bakht O, Pathak P, London E, Effect of the structure of lipids favoring disordered domain formation on the stability of cholesterol-containing ordered domains (lipid rafts): identification of multiple raft-stabilization mechanisms, Biophys J, 93 (2007) 4307–4318. [PubMed: 17766350]

[65]. Silvius JR, Calcium-induced lipid phase separations and interactions of phosphatidylcholine/anionic phospholipid vesicles. Fluorescence studies using carbazole-labeled and brominated phospholipids, Biochemistry, 29 (1990) 2930–2938. [PubMed: 2337575]

[66]. Aston-Mourney K, Hull RL, Zraika S, Udayasankar J, Subramanian SL, Kahn SE, Exendin-4 increases islet amyloid deposition but offsets the resultant beta cell toxicity in human islet amyloid polypeptide transgenic mouse islets, Diabetologia, 54 (2011) 1756–1765. [PubMed: 21484213]

Highlights

- Amyloid formation by the polypeptide hormone IAPP contributes to type-2 diabetes
- Model membranes with high anionic lipid content accelerate IAPP amyloid formation
- High levels of Ca^{2+} reduce anionic membrane catalysed IAPP amyloid formation
- Ca^{2+} effects are modest for membranes with physiological levels of anionic lipids
- Physiological Ca^{2+} levels have modest impact on membrane mediated amyloid formation

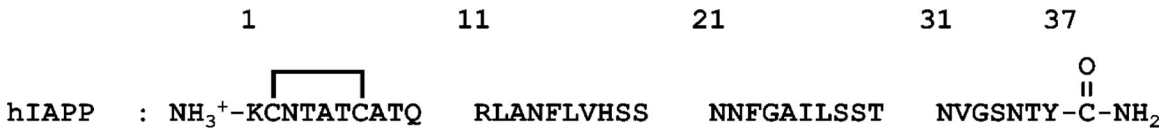

Fig. 1.

Sequence of hIAPP with the disulfide bridge between Cys-2 and Cys-7 and the amidated C-terminus shown.

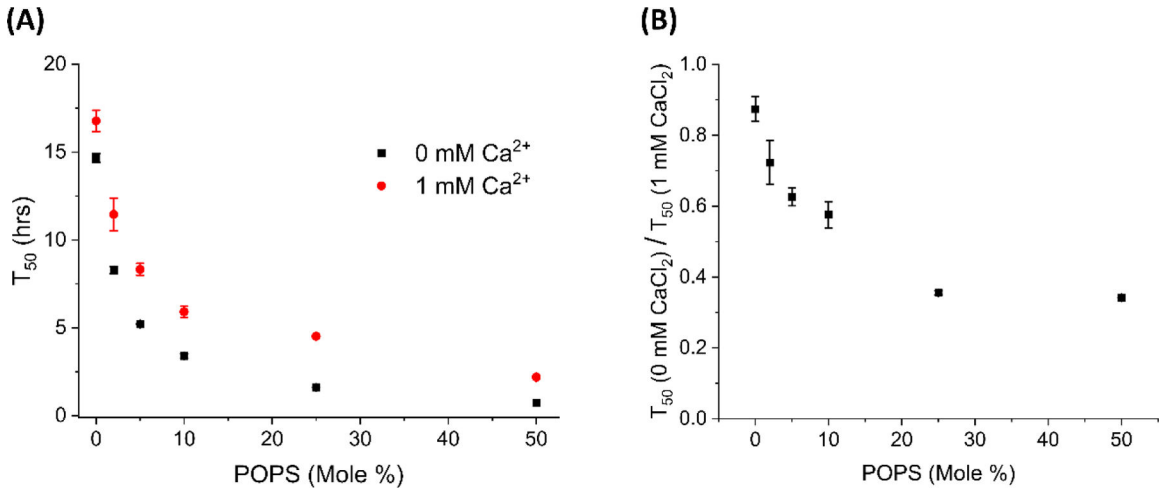

Fig. 2.

Effect of Ca^{2+} upon hIAPP amyloid formation in the presence of vesicles containing different mole % of POPS. (A) T_{50} vs mole % POPS in the presence (red) and absence (black) of 1 mM Ca^{2+}. (B) A plot of the ratio of T_{50} in the absence of Ca^{2+} to T_{50} in the presence of 1 mM Ca^{2+}. Experiments were conducted in 20 mM Tris, 100 mM NaCl, pH 7.4 at 25 °C with 400 μM lipid, 20 μM hIAPP, and 40 μM thioflavin-T. Standard deviations from three experiments are shown and are smaller than the symbols for the data points at 25 mole % POPS and higher.

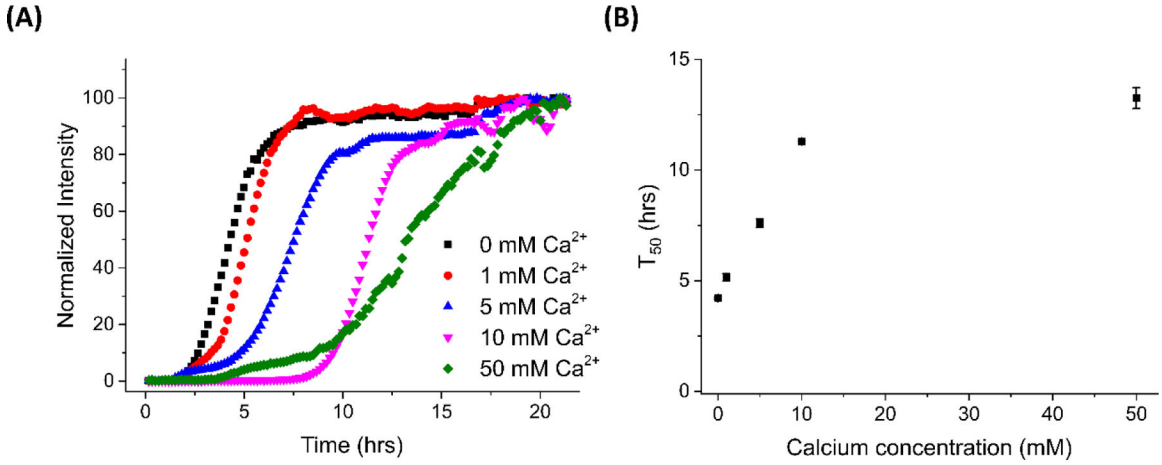

Fig. 3.

hIAPP amyloid formation in the presence of vesicles containing 10 mole % POPS, 90 mole % POPC with different concentrations of Ca^{2+}. (A) Thioflavin-T assays (B) T_{50} of amyloid formation. Experiments were conducted in 20 mM Tris, 100 mM NaCl, pH 7.4 at 25 °C with 400 μM lipid, 20 μM hIAPP, and 40 μM thioflavin-T. Standard deviations from three experiments are shown and are smaller than the symbols except for the 50 mM Ca^{2+} datum point.

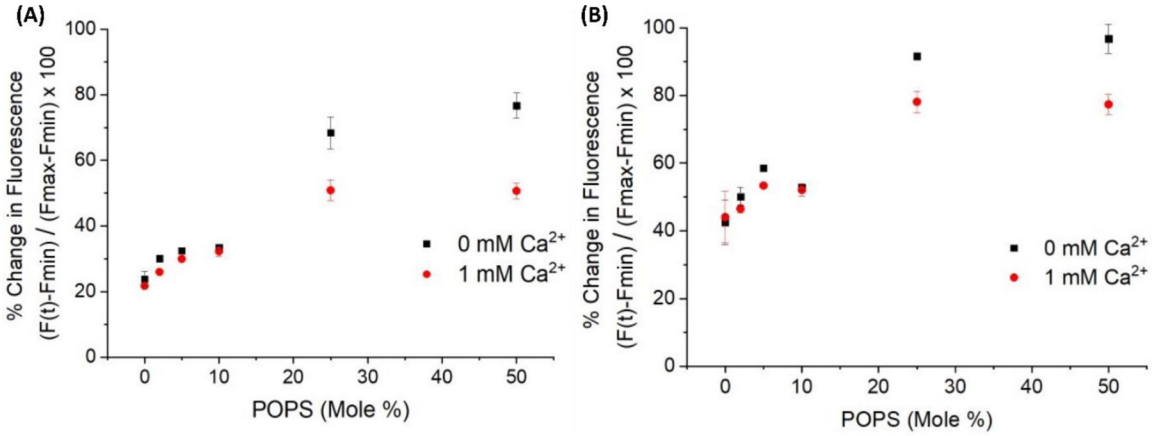

Fig. 4.

The observed % change in fluorescence for carboxyfluorescein leakage assays of hIAPP induced membrane leakage. Experiments were conducted for vesicles containing different mole % of POPS without calcium (black) and with 1 mM calcium (red) at (A) 10 min and (B) 20 hours. Experiments were conducted in 20 mM Tris, 100 mM NaCl, pH 7.4 at 25 °C with 400 μM lipid and 20 μM hIAPP. Standard deviations from three experiments are shown and are smaller than the symbols.

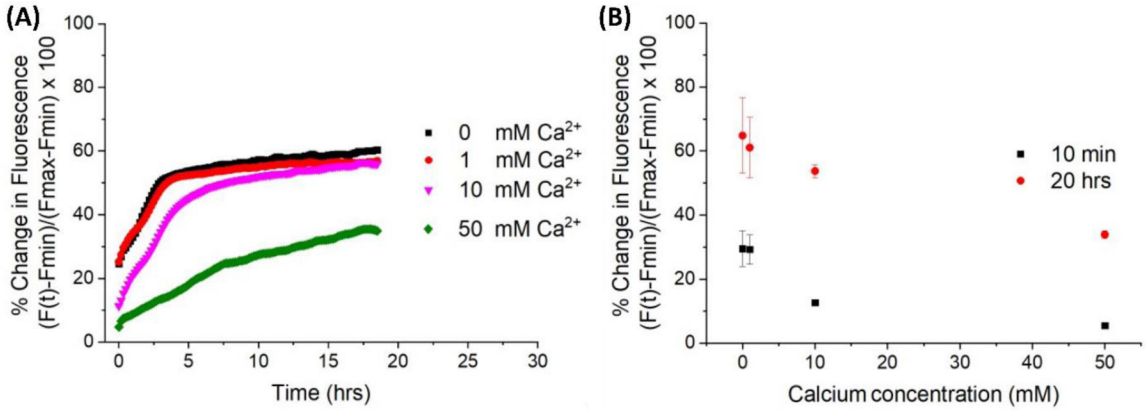

Fig. 5.

The observed % change in fluorescence for carboxyfluorescein leakage assays of hIAPP induced membrane leakage in the presence of vesicles containing 10 mole % POPS, 90 mole % POPC with different concentrations of Ca^{2+}. (A) Kinetics of dye release from vesicle induced by hIAPP. (B) % Leakage at 10 min (black) and 20 hours (red). Experiments were conducted in 20 mM Tris, 100 mM NaCl, pH 7.4 at 25 °C with 400 μM lipid and 20 μM hIAPP. In panel (B), the standard deviations from three experiments are shown and are smaller than the symbols.

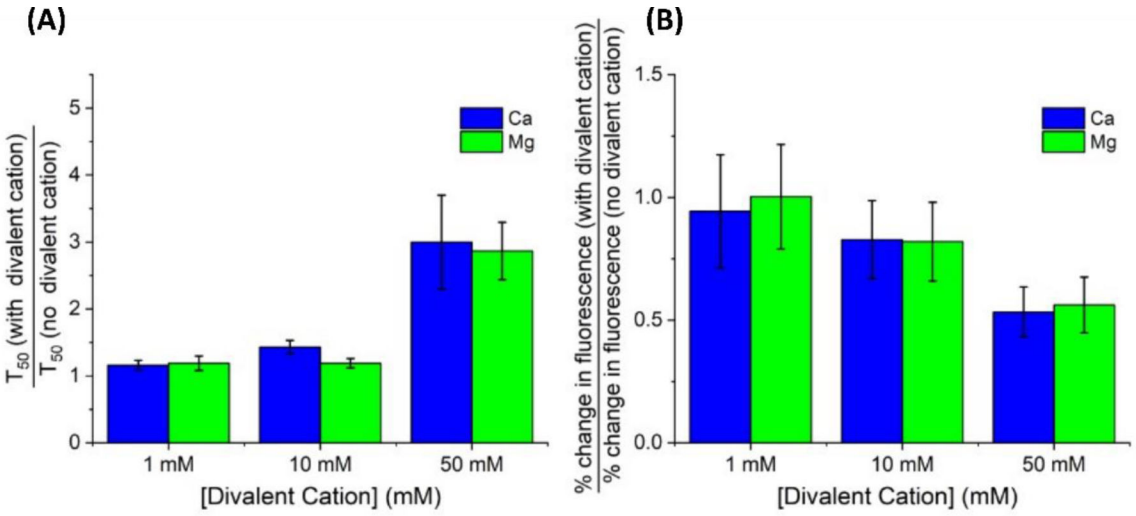

Fig. 6.

Ca^{2+}(Blue) and Mg^{2+} (Green) have similar effects on hIAPP amyloid formation and hIAPP induced LUV leakage. (A) Histogram of the ratio of T_{50} for Thioflavin-T amyloid formation assays conducted in the presence and absence of metal and (B) Histogram of the ratio of hIAPP induced final membrane leakage at 20 hours in the presence and absence of metal. Experiments were conducted with LUVs that contained 10 mole % POPS, 90 mole % POPC LUV and utilized 20 mM Tris, 100 mM NaCl, pH 7.4 at 25 °C with 400 μM lipid and 20 μM hIAPP.

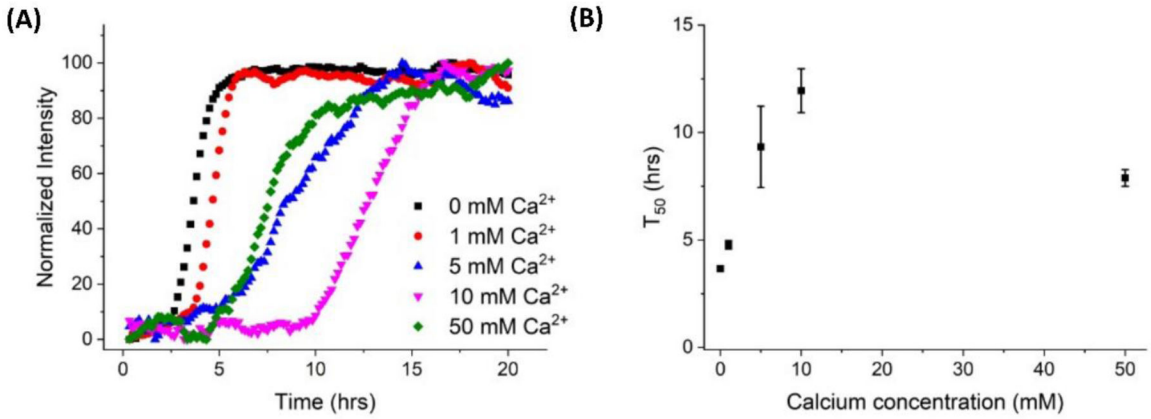

Fig. 7.

Effect of cholesterol on the hIAPP amyloid formation in the presence of Ca^{2+}. (A) Thioflavin-T assays, (B) T_{50} of amyloid formation. Experiments were conducted in 20 mM Tris, 100 mM NaCl, pH 7.4 at 25 °C with 400 μM lipid and 20 μM hIAPP.